

A robust sensor-selection method for P300 brain-computer interfaces.

Hubert Cecotti, Bertrand Rivet, Marco Congedo, Christian Jutten, Olivier Bertrand, Emmanuel Maby, Jérémie Mattout

▶ **To cite this version:**

Hubert Cecotti, Bertrand Rivet, Marco Congedo, Christian Jutten, Olivier Bertrand, et al.. A robust sensor-selection method for P300 brain-computer interfaces.. Journal of Neural Engineering, 2011, 8 (1), pp.016001. 10.1088/1741-2560/8/1/016001 . hal-00584756

HAL Id: hal-00584756
https://hal.science/hal-00584756

Submitted on 11 Apr 2011

HAL is a multi-disciplinary open access archive for the deposit and dissemination of scientific research documents, whether they are published or not. The documents may come from teaching and research institutions in France or abroad, or from public or private research centers.

L'archive ouverte pluridisciplinaire **HAL**, est destinée au dépôt et à la diffusion de documents scientifiques de niveau recherche, publiés ou non, émanant des établissements d'enseignement et de recherche français ou étrangers, des laboratoires publics ou privés.

A Robust Sensor Selection Method for P300 Brain-Computer Interfaces

H. Cecotti [1], B. Rivet [1], M. Congedo [1], C. Jutten [1], O. Bertrand [2], E. Maby [2], J. Mattout [2]

[1] GIPSA-lab CNRS UMR 5216
Grenoble Universities
F-38402 Saint Martin d'Hères, France
[2] INSERM, U821, Lyon, F-69500, France
Institut Fédératif des Neurosciences, Lyon, F-69000, France
Université Lyon 1, Lyon, F-69000, France

Abstract. A Brain-Computer Interface (BCI) is a specific type of human-computer interface that enables the direct communication between human and computers through decoding of brain activity. As such, event-related potentials (ERPs) like the P300 can be obtained with an oddball paradigm whose targets are selected by the user. This paper deals with methods to reduce the needed set of EEG sensors in the P300 speller application. A reduced number of sensors yields more comfort for the user, decreases installation time duration, may substantially reduce the financial cost of the BCI setup and may reduce the power consumption for wireless EEG caps. Our new approach to select relevant sensors is based on backward elimination using a cost function based on the signal to signal-plus-noise ratio, after some spatial filtering. We show that this cost function select sensors subsets that provide a better accuracy in the speller recognition rate during the test sessions than selected subsets based on classification accuracy. We validate our selection strategy on data from 20 healthy subjects.

The corresponding author is:
Hubert Cecotti
email: hub20xx@hotmail.com

Submitted to: *J. Neural Eng.*

1. Introduction

A Brain-computer interface (BCI) is a direct communication pathway between a human brain and an external device. It enables people to communicate through the direct and real-time measurements of brain activity, without requiring any peripheral (muscular) activity [1]. BCIs may represent the only communication pathway for patients who are unable to communicate via conventional means because of severe motor disabilities like spinal cord injuries or amyotrophic lateral sclerosis (ALS) [2]. Hence BCIs are presented as a promising system to restore control and communication in some patients [3].

Nowadays, one important challenge is to reduce the number of electrodes in an optimal fashion for each user. Reducing the number of sensors yields more comfort for the user, decreases installation time duration and may substantially reduce the financial cost of the BCI setup since the cost of an EEG cap and an amplifier vary in relation to the number of channels. Besides, the reduction of the number of sensors can also reduce the power consumption for wireless EEG caps [4]. Finally sensor selection could improve the accuracy of P300 detection by selecting a reduced and more relevant set of input features by removing irrelevant featues and by avoiding overfitting. Pattern recognition and signal processing techniques are usually used in BCI for both detection and classification of specific brain signals. Among these techniques, machine learning models [5, 6, 7, 8] have been proved quite efficient. In addition to knowledge in neuroscience and neurophysiology that guide the process of signal extraction, machine learning techniques allow modeling signal variability across subjects and over time. Neural networks [9, 10, 11, 12, 13, 14], support vector machines [15, 16], linear discriminant analysis (classical, stepwise, Bayesian) [17, 18] and hidden Markov models [19, 20] have already been applied to BCI and EEG data classification. For these techniques, the choice of an optimal set of input features can be decisive for the classification performance. Hence feature selection serves several purposes: to improve the classifier accuracy, to adapt to the user and to reduce the general BCI cost for the user/patient both in terms of financial and attentional efforts.

We distinguish sensor selection and feature selection. Indeed, a sensor generally corresponds to a set of features. It is the case in BCI where an input signal often corresponds to a matrix with one dimension in the space domain (sensors) and the other one in the time or frequency domain. This paper will focus on sensor selection.‡

Several strategies exist for selecting a subset of sensors. For instance, one can select sensors based on prior knowledge from the literature or previous experiments. In that case, the subset is fixed and may jeopardize the performance in some subjects as the optimal sensor subset is highly subject-dependent [17]. Therefore, it is mandatory to identify subject-specific optimal sensor subsets. For a N sensors set, there are 2^N different possible subsets. To find the optimal subset, three main searching approaches can be considered: complete, random or sequential search. The complete (exhaustive)

‡ In the following parts, we consider the sensors as the sensors that provide the signal, as opposed to sensors dedicated to the reference and ground.

search is usually intractable as the search space is often exponentially prohibitive. The random search starts with a randomly selected subset and add randomness in the sequential approach or generates new random subsets as with the Las Vegas algorithm [21]. Finally, the sequential search does not guarantee optimality as it gives up completeness. However, it is easily implementable and can provide optimal solutions given some evaluation criterion. Several variations are described in the literature like the greedy hill-climbing approach, forward selection, backward elimination or bi-directional selection. For instance, Recursive Feature Elimination was used for sensor selection in BCI based on motor imagery [22, 23].

In this paper, we consider a backward elimination strategy to address the following issues: to find an efficient criterion to exclude the least relevant sensors; or equivalently, to evaluate the relevance of a given sensor subset. The effect of sensor selection then needs to be evaluated on the P300-speller performance.

The rest of the paper is organized as follows. The P300-speller paradigm is described in the next section. The sensor selection strategy and the different criteria for sensor evaluation are described in the third section. Section four is dedicated to the computation of the spatial filtering, the signal to signal-plus-noise ratio and the P300 classifier. The experimental design is presented in the fifth section. Results of sensor selection based on different criteria are compared and discussed in the last two sections.

2. P300 speller

The P300-speller enables a user to write symbols (letters, digits,...) on a computer screen. This BCI is based on the following principle: a matrix containing all the available symbols is displayed on screen [24, 25]. In the experiments, we consider a 6×6 matrix, as used in classical P300 spellers [24]. To spell a symbol, the user has to focus her/his attention on the character she/he wants to spell. The rows and columns of the matrix are alternatively and randomly intensified. Hence the intensification of the target is a rare and unexpected event, which causes a P300 time-locked EEG response (a positive voltage deflection at latency of about 300ms). Stimulation is organized in block of 12 flashes such that each row/column is intensified once per block§. Blocks of 12 intensifications are repeated N_{epoch} times for each symbol. Therefore, $2 \times N_{epoch}$ P300 responses might be detected to identify the target.

The P300-speller is made of two classification steps: first, signal classification that aims at identifying a P300 response from other responses in the EEG streaming data; second, the decision about what was the target based on the classifications of the row and column signals respectively. These two steps are sequential. Detection of a P300 response corresponds to a binary classification (present/absent). This step usually requires averaging over several epochs since a drop of attention may prevent a P300 response to occur. Besides, the background EEG and movements or other artefacts might impair the detection performance. In the symbol recognition step, the outputs of

§ One block thus corresponds to intensification of the six rows and six columns in a random fashion.

the P300 classification are combined to make a final decision. The target is defined by a single row/column pair. We note $V \in \mathbb{R}^{12\times N_{epoch}}$ the matrix containing the cumulated probabilities of a P300 detection for each intensification (or flash) and each epoch:

$$V(i,j) = \sum_{k=1}^{j} E_{P300}(P(i,k)) \tag{1}$$

where $P(i,k) \in \mathbb{R}^{N_f \times N_e}$ is the response pattern to the flash i, at epoch k, $(i,k) \in \{1,\ldots,12\} \times \{1,\ldots,N_{epoch}\}$. N_f and N_e indicate the number of virtual sensors and the number of sampling points in the extracted signal to process, respectively. Finally, $E_{P300}(.)$ is a classifier returning a confidence value $v \in [0,1]$: 1 (resp. 0) denotes a perfect confidence that a P300 response is present (resp. absent).

At each epoch j, one can evaluate the coordinate (x_j, y_j) of the selected symbol by:

$$x_j = \text{argmax}_{\ 1\leq i\leq 6} V(i,j) \tag{2}$$

$$y_j = \text{argmax}_{\ 7\leq i\leq 12} V(i,j). \tag{3}$$

We denote by $E_{Speller}(\{P(1,N_{epoch}),\ldots,P(12,N_{epoch})\}) = (row, column)$, the selected symbol.

3. Sensor selection

3.1. Backward elimination

The chosen method for adaptively selecting a relevant subset of sensors is based on backward elimination. Starting with all sensors, it consists in alternatively testing each sensor for its significance and in removing the least relevant one at each iteration step. An irrelevant sensor is a sensor whose removal barely impairs the performance or selection criterion. In this work, we eliminate two sensors at a time, leaving us with the most significant remaining subset. Elimination goes on until every sensor has been eliminated. At the end of the process, sensors can be ranked according to their revealed significance. Basically, a relevant sensor will be eliminated at the end of the iterative process while a useless one will be eliminated along the very first iterations. The rank of a sensor $R(s)$ is defined by $N_s/2 - i$ where i is the iteration where the sensor has been removed and N_s is the number of sensors. As a consequence, the higher the rank of a given sensor is, the more relevant the sensor is.

3.2. Subset evaluation

The distinction between dependent and independent selection criteria to establish the performance or score of a given subset of sensors is important. Dependent criteria rely on a subsequent measure of classification accuracy to establish the relevance of a given subset, while independent criteria do not. Therefore, a dependent criterion might be more suitable given the ultimate goal of the task but is often computationally more

expensive since measuring classification accuracy for a large number of possible subsets calls for a cumbersome K-fold cross-validation procedure. Instead, independent criteria can be based on simple measures of the goodness of fit of the extracted signal features, like information measures, distance measures, dependency measures or consistency measures [26]. In the P300-speller, subset evaluation can be assessed at three different levels: *(i)* a global measure of the EEG signal (*e.g.*, Signal to Noise Ratio (SNR) or Signal to Signal plus Noise Ratio (SSNR), *(ii)* the recognition rate of the P300 response (E_{P300}), *i.e.,* how well the P300 is detected individually, and *(iii)* the accuracy of the speller ($E_{Speller}$). Those criteria can be compared, whether pre-processing include some spatial filtering (SF) or not. We distinguish four main criteria for the evaluation that are presented hereafter.

3.3. Criterion based on the SSNR

The first criterion is based on the SSNR. We consider an analytical model of the recorded signals X that is composed of three parts: the P300 responses (D_1A_1), a response related to every superimposed evoked potentials (D_2A_2) and the residual noise (H)

$$X = D_1A_1 + D_2A_2 + H. \tag{4}$$

where $X \in \mathbb{R}^{N_t \times N_s}$, N_t and N_s are the number of sampling points over time and the number of sensors, respectively. $A_1 \in \mathbb{R}^{N_e^1 \times N_s}$ and $A_2 \in \mathbb{R}^{N_e^2 \times N_s}$ are the matrices of ERP signals. N_e^1 and N_e^2 are the number of sampling points that describe the P300 response and the superimposed evoked potentials, respectively. In the following parts, N_e^1 and N_e^2 are chosen to correspond to 0.6 second. D_1 and D_2 are two real Toeplitz matrices of size $N_t \times N_1$ and $N_t \times N_2$ respectively. D_1 has its first column elements set to zero except for those that correspond to a target, which are represented with a value equal to one. For D_2, its first column elements are set to zero except for those that correspond to stimuli onset. N_1 and N_2 are the number of sampling points representing the target (the P300 response) and superimposed evoked potentials, respectively. H is a real matrix of size $N_t \times N_s$.

The SSNR is defined by :

$$\text{SSNR} = \frac{Tr(\hat{A}_1^T D_1^T D_1 \hat{A}_1)}{Tr(X^T X)} \tag{5}$$

where $\hat{A}_1$ corresponds to the least mean square estimation of A_1.

$$\hat{A} = \begin{bmatrix} \hat{A}_1 \\ \hat{A}_2 \end{bmatrix} = ([D_1; D_2]^T [D_1; D_2])^{-1} [D_1; D_2]^T X \tag{6}$$

where $[D_1; D_2]$ is a matrix of size $N_t \times (N_1 + N_2)$ composed of D_1 and D_2.

3.4. Criterion based on the signal power

The power $\mathcal{P}(i)$ of the P300 across the signal on the i^{th} sensor s_i is estimated by:

$$\mathcal{P}(i) = \hat{a_1}^T(i) D_1^T D_1 \hat{a_1}(i) \tag{7}$$

where $1 \leq i \leq N_s$ and $\hat{A}_1 = [\hat{a_1}(i), \ldots, \hat{a_1}(N_s)]$. The power over the $\mathcal{P}$ of the P300 over the signal is defined by:

$$\mathcal{P} = \sum_{i=1}^{N_s} \mathcal{P}(i). \tag{8}$$

3.5. Criterion based on the P300

We define the criterion based on the P300, Acc_{P300}, as the average recognition rate of the P300 classifier across the different epochs, every intensification of the row/column and the total number of symbols to spell (N_{symb}). The recognition rate of the classifier takes also into account the fact that a non P300 signal must not be recognized as a P300. The Bayesian linear discriminant analysis (BLDA) is used here for the binary classification of P300 and no P300 responses [17, 27].

3.6. Criteria based on the speller accuracy

Finally, the criterion based on the recognition rate of character for the P300 speller, $Acc_{Speller}$, is related to the application. $Acc_{Speller}$ is defined as the average recognition rate over every epoch. This criterion is not the speller accuracy for a specific epoch: it takes into account every repetition to provide a more detailed measure. Indeed, if we consider the accuracy for a particular number of epochs, this value may not vary so much with a small database of characters. It is worth mentioning that to compute the speller accuracy, every step for computing the P300 accuracy are also needed. This definition of an average accuracy is used as a criterion for sensor selection. Later, in the evaluation of the P300 speller during the test phase, classification accuracy will be computed for a specific number of epochs.

4. Spatial filters

The criteria defined in section 3.3, 3.4, 3.5 and 3.6 can be combined with spatial filters for enhancing the signal. Spatial filters are one of the first steps for processing the signal in order to enhance its peculiar characteristics. Several types are described in the literature. For fixed spatial filters, the weights for each sensor are fixed manually. For instance, with the average combination, each electrode has the same weight. A common approach is to use a bipolar or Laplacian combination of the sensors for canceling the common noise signals [28]. Adaptive spatial filters usually consider statistical methods like ICA [29] and Common Spatial Pattern (CSP) [30, 31, 32, 33, 34]. The filters are obtained by solving a generalized eigenvalue problem. Spatial filters can also be set with a generative approach. Such filters are set as a function of the expected signal to detect, like the minimum energy combination and the maximum contrast combination [35]. Finally, spatial filters can be directly embedded in the classifier as described in [10].

The considered method for the creating spatial filters is based on the xDAWN algorithm [36, 37]. This method assumes two hypotheses. First, there exists a typical

response synchronized with the target stimuli superimposed with an evoked response by all the stimuli (target and non-target). Second, the evoked responses to target stimuli could be enhanced by spatial filtering.

We consider spatial filters $U_1 \in \mathbb{R}^{N_s \times N_f}$ to enhance the signal to signal-plus-noise ratio (SSNR) of the enhanced P300 responses ($D_1 A_1 U_1$), where N_f is the number of spatial filters

$$XU_1 = D_1 A_1 U_1 + D_2 A_2 U_1 + HU_1. \tag{9}$$

We define the SSNR in relation to the spatial filters by:

$$\text{SSNR}(U_1) = \frac{Tr(U_1^T \hat{A}_1^T D_1^T D_1 \hat{A}_1 U_1)}{Tr(U_1^T X^T X U_1)} \tag{10}$$

The SSNR is maximized by:

$$\hat{U}_1 = \text{argmax}_{\ U_1}\ \text{SSNR}(U_1). \tag{11}$$

The procedure for computing $\hat{U}_1$ and $\text{SSNR}(U_1)$ are detailed in the appendix. The enhanced signal can be computed by:

$$\hat{X} = X\hat{U}_1. \tag{12}$$

The power of the filtered signal is determined by:

$$PU = Tr(U_1^T \hat{A}_1^{\ T} D_1^T D_1 \hat{A}_1 U_1^T) \tag{13}$$

which is equal to the SSNR of the enhanced signal multiplied by N_f.

5. Experiments

5.1. Objectives

The objectives of the experiments are to evaluate and compare different evaluation criteria that we have considered for backward elimination. These criteria are summarized in Table 1. The criteria defined in section 3.3, 3.4, 3.5 and 3.6 are applied without ($C1$, $C2$, $C3$, $C4$) or with ($C1_{SF}$, $C2_{SF}$, $C3_{SF}$, $C4_{SF}$) spatial filtering (SF) as preprocessing. $C1$ and $C1_{SF}$ rely on the signal to signal-plus-noise ratio (SSNR). $C1$ and $C1_{SF}$ are defined in Eq. (5) and (A.3), respectively. $C2$ and $C2_{SF}$ rely on the signal power defined in Eq. (8) and (13), respectively. As $C1_{SF}$ and $C2_{SF}$ are equivalent, we will only mention $C1_{SF}$ in the next sections. $C3$ and $C3_{SF}$ are based on the classification accuracy of the P300 responses (Acc_{P300}) defined in section 3.5 and $C4$ and $C4_{SF}$ rely on the classification accuracy of symbol recognition ($Acc_{Spelle r}$) defined in section 3.6. Note that the latter involves classification of the P300 responses. And the more steps required by a criterion, the higher the computational cost. The challenge here is to determine the best criterion for selecting an optimal subset of sensors, given a desired number of sensors.

$C1$:			SSNR
$C2$:			Power
$C3$:			Acc_{P300}
$C4$:			$Acc_{Speller}$
$C1_{SF}$:	SF	+	SSNR
$C2_{SF}$:	SF	+	Power
$C3_{SF}$:	SF	+	Acc_{P300}
$C4_{SF}$:	SF	+	$Acc_{Speller}$

Table 1. The various criteria for backward selecting the more relevant sensors.

5.2. Data acquisition

The EEG signal was recorded on 20 healthy subjects (13 males, 7 females) with the OpenViBE framework [38]. The average age is 26 years, with a standard deviation of 5.7. Subjects were wearing an EEG cap with 32 electrodes [39]. The EEG activity was recorded continuously from 32 active electrodes (actiCap, Brain Products GmbH, Munich). The electrodes for reference and the ground were placed on the nose and on the forehead, respectively. For testing the different subset evaluations methods, we consider four sessions: one for training the classifier, the others for testing. The sessions have the following parameters:

- Training session : 50 characters with 10 epochs.
- Test session 1: 60 characters with 5 epochs.
- Test session 2: 60 characters with 8 epochs.
- Test session 3: 60 characters with 10 epochs.

5.3. Pre-processing

The EEG signal was sampled at 100Hz. As preprocessing, time series were bandpass filtered between 1Hz and 12.5Hz with a Butterworth filter (order=4) and resampled down to 25Hz. For each sensor, the signals were then normalized so that they had a zero mean value and a standard deviation equal to one.

5.4. Off-line classification accuracy

The P300-speller is evaluated with different sensor subsets as defined in the previous section. For each sensor subset, the signal was enhanced by using the spatial filters presented in Eq. (A.4). The BLDA classifier described in section 3.5 is used for the detection of the P300. Only the four first components of the enhanced signal are considered. It is worth noting that the number of components depends on the number of selected sensors ($N_f = 4$ if $N_s \geq 4$ and $N_f = N_s$ otherwise).

The purpose of the off-line classification is to prove: *(i)* the efficiency of the spatial filtering method for selecting sensors, *(ii)* compare the efficiency of the different criteria,

(iii) prove the interest of $C1_{SF}$ that provides in one step the spatial filters and the SSNR.

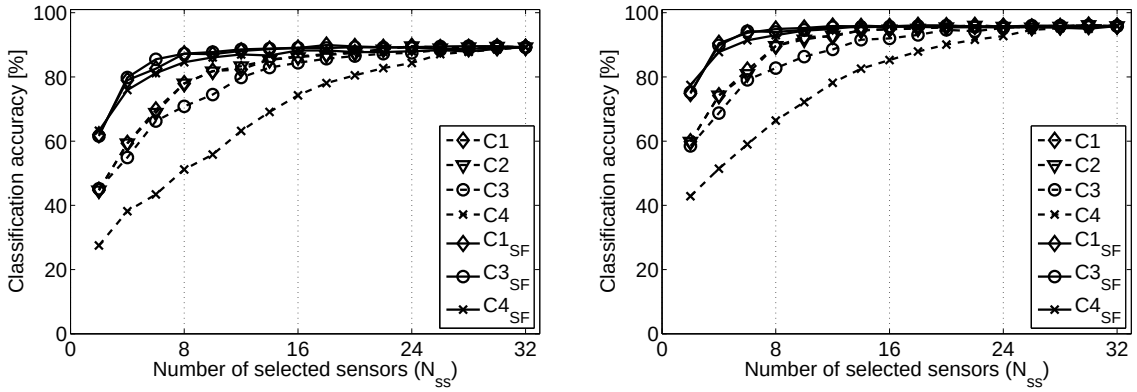
6. Results

6.1. Global speller accuracy

In the P300-Speller scenario, the speller accuracy is the most important criterion for determining the efficiency of the methods for selecting sensors. Figure 1 presents the accuracy on the session 3 of the test database (10 epochs), for each subset evaluation method and different sizes of the subset. The selection methods that do not consider the spatial filters provide the worst results (*e.g.*, between 66.42% ($C4$) and 89.58% ($C1$) for a subset of eight sensors). With eight sensors, the average recognition rate of the speller is 94.92%, 94.00% and 93.00% when using $C1_{SF}$, $C3_{SF}$ and $C4_{SF}$ respectively. The latter performances suggest that sampling down to eight suitably selected sensors does not impair the recognition rate significantly. Indeed, the highest accuracy for the speller is obtained with 32 sensors, it reaches 95.83% of good detection. Importantly, spatial filtering proves essential in performing a relevant sensor selection. When sampling down to eight sensors, it improves the speller accuracy by 5.34%, 11.25% and 26.58% for $C1_{SF}$, $C3_{SF}$ and $C4_{SF}$ respectively. This also suggests that the criterion based on the SSNR is less dependent upon the spatial filters.

It also proves that spatial filtering has a critical impact on the selection of suitable sensors. Finally, $C1_{SF}$ is sufficient for creating suboptimal sets of sensors. The performance gap between $C1_{SF}$ and $C3_{SF}$ is rather small and it is not possible to rank these methods based on the selected sensor subsets. The computational cost is indeed less important with $C1_{SF}$. This criterion based of the SSNR evaluation with spatial filtering as preprocessing ($C1_{SF}$) can be done in one step thanks to the xDAWN algorithm. It avoids considering further steps like the Acc_{P300} ($C3_{SF}$) or $Acc_{Speller}$ ($C4_{SF}$), which increase the complexity of the sensor selection procedure and provide slightly less relevant sensors. The criteria based on the speller accuracy provide the worst results. These results can be explained by the low number of symbols that is taken into account for the evaluation of the speller accuracy. In addition, the speller accuracy is based on the intersection of the several detected P300. It is possible to not recognize correctly a symbol but by having correctly recognized individually the row or the column. The speller accuracy therefore yields to a less precise estimation of the P300 detection.

The accuracy of the P300 speller in relation to the number of epochs is presented in Fig. 2. The more epochs are used, the more the speller accuracy increases. However, the speller accuracy remains acceptable till about five epochs. The best performance is always produced with $C1_{SF}$ and $C3_{SF}$ with 87.08% and 87.75 % respectively, with five epochs.



(a) 5 epochs (b) 10 epochs

Figure 1. Accuracy of the P300 speller in relation to the number of selected sensors.

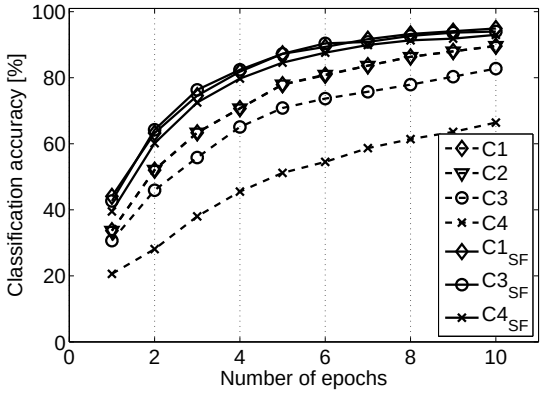


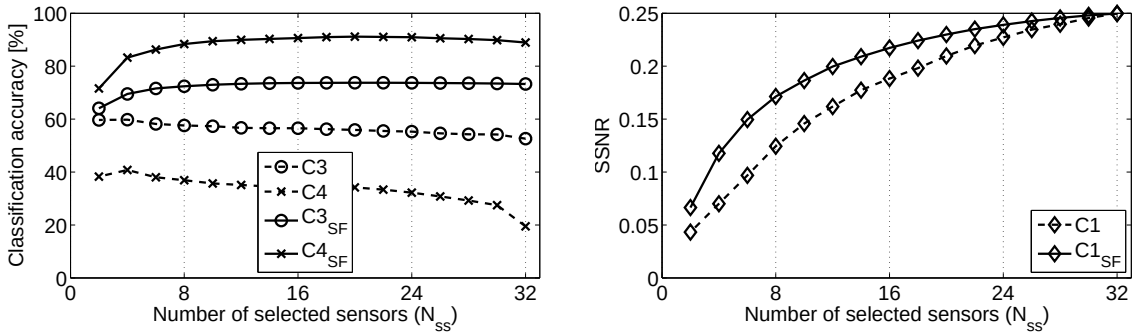
Figure 2. Accuracy of the P300 speller in relation to the number of epochs, for eight selected sensors.

6.2. Effect of spatial filtering

The evolution of each sensor selection criterion defined in section 3.2 over the number of selected sensors is presented in Fig. 3. For Fig 3(a), the classification accuracy is calculated with the function defined in sections 3.5 and 3.6 for criteria ($C3$, $C3_{SF}$) and ($C4$, $C4_{SF}$), respectively. As expected, the selection criterion value decreases in relation to the number of remaining sensors in the backward elimination for $C3_{SF}$ and $C4_{SF}$. In addition, the values of $C3_{SF}$ are always inferior to $C4_{SF}$, showing the difficulty to reach a high accuracy for the P300 detection. Yet, we observe the inverse behavior when there is no spatial filters, *i.e.* for $C3$ and $C4$. The large number of input features compared to the low number of training samples is probably the cause of this behavior. With spatial filtering as preprocessing, feature reduction improves the accuracy for the selected classifier by avoiding overfitting of training data.

In Fig 3(b), the evolution of the values for $C1$ and $C1_{SF}$ also decreases in relation to the number of remaining sensors during the backward elimination. In addition, it shows that spatial filtering reduces the influence of the noise and allows keeping the

SSNR higher while decreasing the number of sensors. The impact of the spatial filters is higher when the number of remaining sensors is low as the gap between $C1$ and $C1_{SF}$ is large. With the sensor selection used with $C1$, the sensors with the worst SSNR are removed at each iteration. This greedy strategy that focuses on the SSNR of each sensor is not optimal. Besides, the performance between $C1$ and $C2$ is almost equivalent.



(a) Recognition rate (b) SSNR

Figure 3. Evolution of the different criteria in relation to the number of selected sensors.

6.3. SSNR analysis

When selecting a set of sensors, it is tempting to focus only on the sensors with the highest SSNR. Actually, the sensors that are removed during the backward elimination with the method $C1$ do not provide the best SSNR of the obtained subset. This observation indicates that the best sensor subset does not only contain the sensors with the best SSNR. Spatial filtering proves the efficiency of a global approach for evaluating the SSNR. This part deals with the relationships between spatial filtering, SSNR, and sensor selection. In Figure 4, the evaluation of the different subsets extracted with $C1$ and $C1_{SF}$ are compared with the two evaluation methods of the SSNR: before and after spatial filtering, *i.e.* with Eq. (5) and Eq. (A.3). Figure 4 allows the evaluation of the impact of the best spatial filter on the SSNR for two fixed set of sensors. It is worth noting that only the filter maximizing the SSNR is considered here, contrary to figure 3(b). For $C1$ and $C1(SF)$, like for $C1_{SF}$ and $C1_{SF}(SF)$, the SSNR are evaluated on the same set of sensors (same number of sensors and same locations). As expected, spatial filtering increases the SSNR as defined in Eq. (A.3). Without spatial filtering, the subsets obtained with criterion $C1$ provide the best results as these subsets were set in relation to the SSNR before applying spatial filtering. Before spatial filtering, the less sensors are considered, the better the SSNR is increased. Indeed, the sensor selection procedure improves the global SSNR by removing sensors, which contain a lot of noise and few relevant information. For both criteria, the SSNR increases with the use of spatial filtering $C1(SF)$ and $C1_{SF}(SF)$, compared to $C1$ and $C1_{SF}$ respectively. In addition, the subsets of sensors selected with $C1_{SF}$ yields to the best SSNR after spatial

filtering: whereas the method $C1$ selects sensors with the best SSNR before spatial filtering, the method $C1_{SF}$ selects sensors by maximizing enhanced SSNR, *i.e.* with spatial filtering. Whereas the subsets obtained with $C1_{SF}$ provide lower SSNR before spatial filtering compared to the subsets given by $C1$, the gain obtained with spatial filtering is greater for $C1_{SF}$ than for $C1$. Indeed, by maximizing the SSNR after spatial filtering ($C1_{SF}(SF)$), the noise impact is taken into account. Method $C1_{SF}$ selects sensors with lower SSNR before spatial filtering than the method $C1$, however these sensors allow increasing the relevance of the informative sensors after spatial filtering. This means that a strategy based on the elimination of the sensors with the worst SSNR before spatial filtering leads to remove sensors that could have helped at improving the SSNR of the whole sensor set.

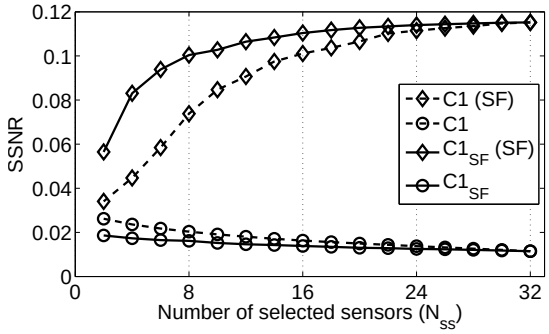


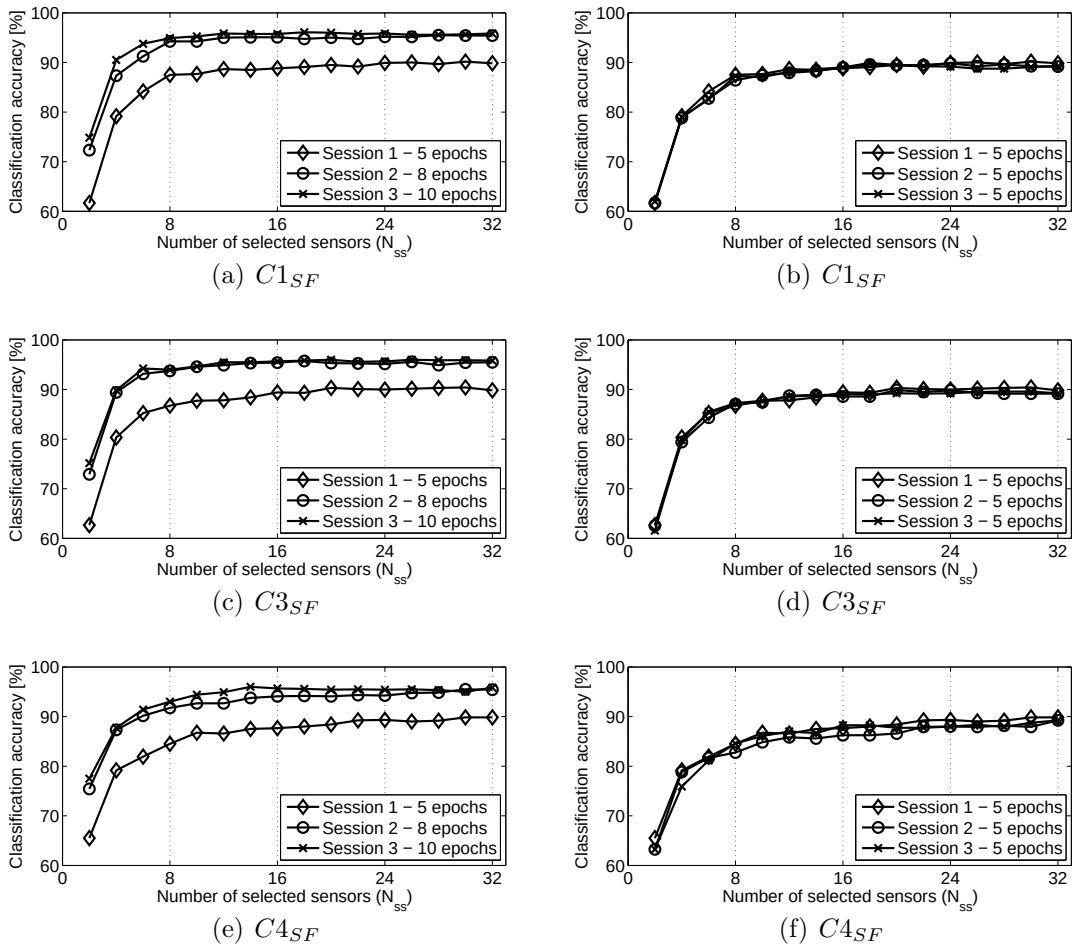
Figure 4. Evolution of the SSNR with and without spatial filtering (SF) in relation to number of selected sensors (N_{ss}) for the selection method $C1$ and $C1_{SF}$.

6.4. Speller accuracy across sessions

We evaluate the accuracy of the speller for three sessions in relation to the number of selected sensors, as depicted in Fig. 5, to check the robustness of the selected sensors across sessions. In the left column, the number of epochs is different for each session. The difference between 8 and 10 epochs is relatively small. However, using only 5 epochs involves a drop in the performance. For instance, the performance between 10 and 5 epochs decreases in average of 7.42%. In the second column, we limit the evaluation till 5 epochs for evaluating the stability of the method across the sessions. For $C1_{SF}$ and $C3_{SF}$, the performance is stable between the three sessions. Though, we observe more differences with $C4_{SF}$, showing that the criterion based on the application is not very robust.

6.5. Sensor rank analysis

For a better understanding of the sensor selection impact across subjects, we propose to analyze the differences and similarities of selected sensors for each subject (Fig. 6). This figure contains the mean of the rank over every subject (a). We define a binary rank $R_2(s)$ that is equal to one if the sensor s is selected, zero otherwise. The mean,



(a) $C1_{SF}$ (b) $C1_{SF}$

(c) $C3_{SF}$ (d) $C3_{SF}$

(e) $C4_{SF}$ (f) $C4_{SF}$

Figure 5. Accuracy of the P300 speller across different sessions. The criterion is $C1_{SF}$ for (a,b), $C3_{SF}$ for (c,d) and $C4_{SF}$ for (e,f).

the standard deviation (S.D.) and the kurtosis of R_2 across the 20 subjects with eight selected sensors are depicted in Fig. 6 in the column (b), (c) and (d) respectively. Like for the previous figures, a dark (resp. light) graylevel denotes a high (resp. low) rank. The first column represents the mean for every subject and sensor, without normalization. The average sensor selection is very similar between the method $C1_{SF}$ and $C3_{SF}$, with a clear selection of P_z, O_z, and P_8. The same remark arises with the normalized rank R_2 (b) in Fig. 6, which restricts itself to the mean across subjects for the subset of eight electrodes. P_z, O_z and P_8 are selected at the three most common sensors for both $C1_{SF}$ and $C3_{SF}$. Indeed P_z, O_z and P_8 are selected 14, 13 and 14 times (resp. 14, 15 and 14 times) for $C1_{SF}$ (resp. $C3_{SF}$) across the 20 subjects. For $C4_{SF}$ the ideal sensor placement is more heterogeneous. It is challenging to extract some sensors that may be useful for every subject. For $C4_{SF}$, the S.D. of the sensor rank is at around 0.4 for most of the sensors. For $C1_{SF}$ and $C3_{SF}$, the S.D. is low on the frontal area as these sensors are almost never selected. However, the S.D. is higher in the occipital and parietal area, suggesting that the order of these sensors can vary a lot while keeping a high rank in

the selection. Finally, the figures of the last column (d) aim at depicting the sensors that could be relevant for few subjects. The kurtosis of the sensor rank suggests that although the majority of the relevant sensors are in the occipital and parietal area, some sensors in the frontal area remain important for some subjects. This observation proves the necessity to personalize the sensor location for optimal performance. Figure 7 presents the sensor rank and the different P300 waves on each sensor, starting after the flash and during 0.6s, for three subjects. The P300 waves are estimated in $\hat{A}_1$. These results highlight the differences of sensor subsets and the P300 curves on each sensor.

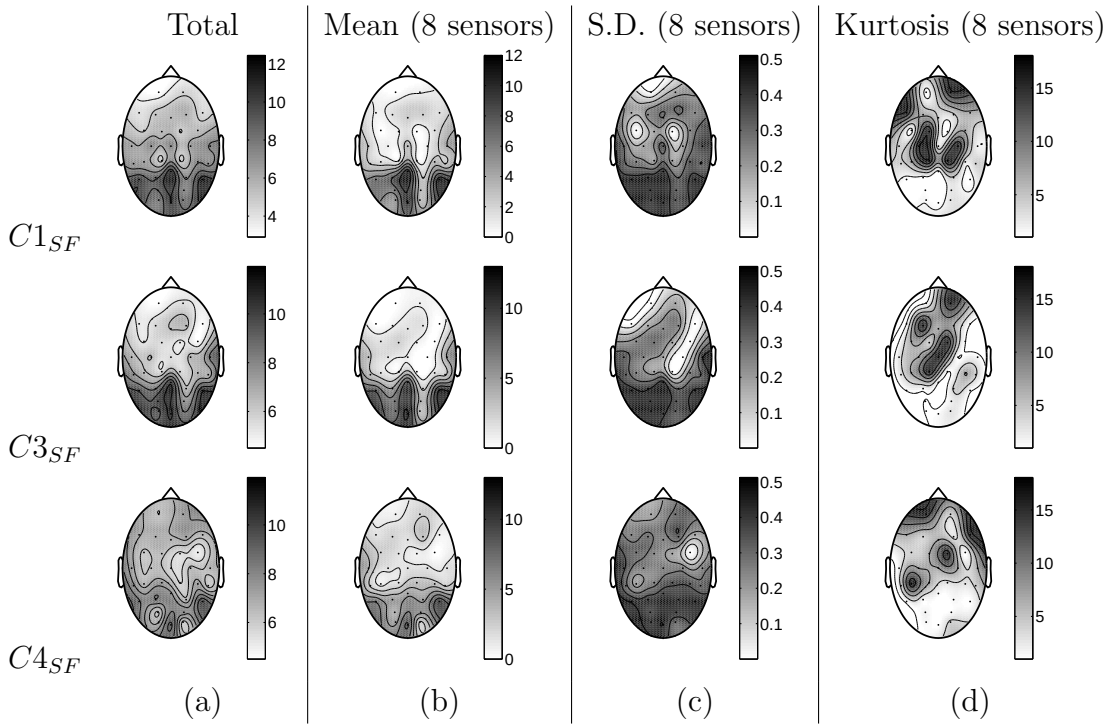
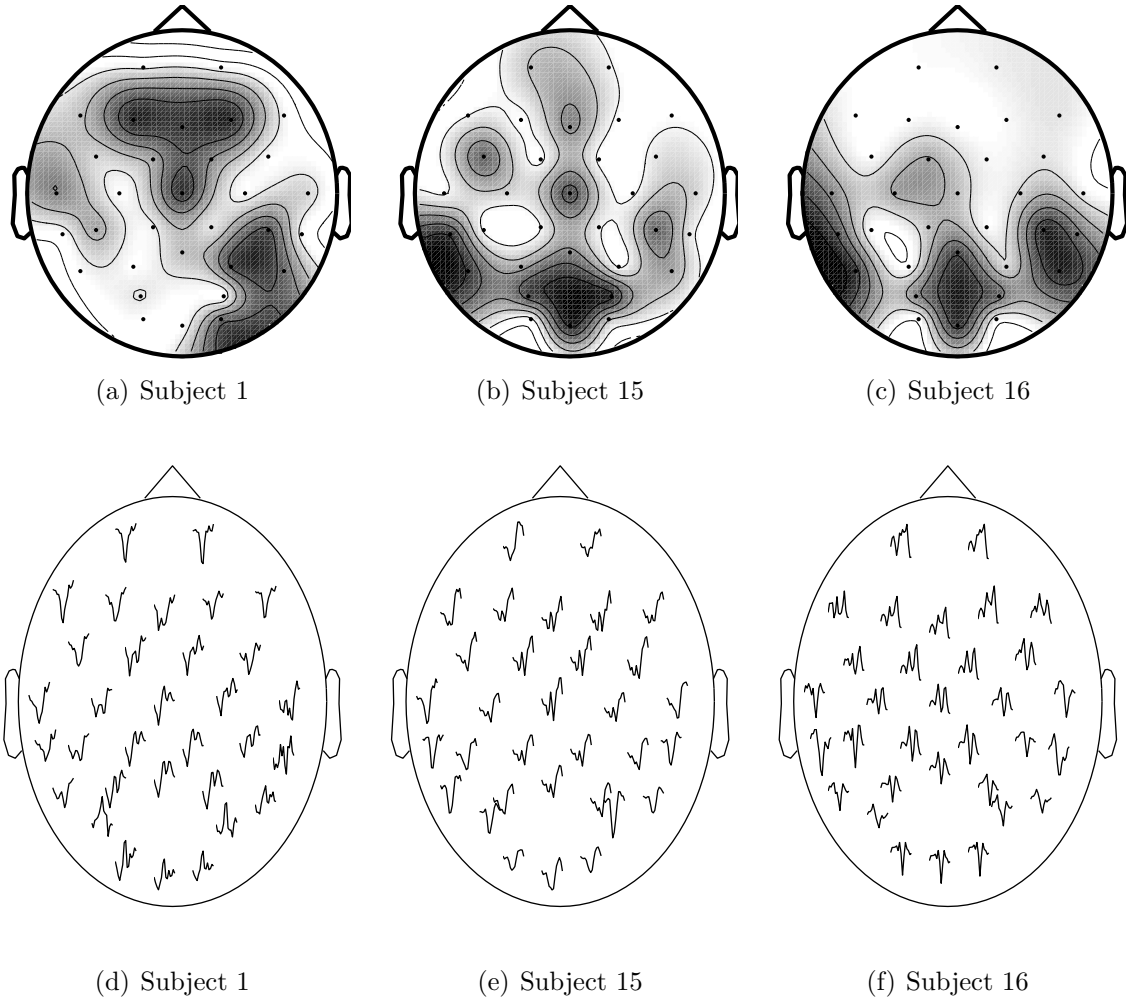


Figure 6. Global rank for every sensor.

Rank	1	2	3	4	5	6	7	8
$C1_{SF}$	$P_Z; 14$	$P_8; 14$	$O_Z; 13$	$P_3; 11$	$P_7; 10$	$PO_9; 9$	$O_1; 9$	$CP_6; 7$
$C3_{SF}$	$O_Z; 15$	$P_Z; 14$	$P_8; 14$	$P_7; 12$	$O_1; 12$	$PO_9; 10$	$T_8; 9$	$P_3; 9$
$C4_{SF}$	$P_8; 13$	$O_Z; 11$	$P_7; 9$	$P_Z; 8$	$F_4; 7$	$P_3; 7$	$P_4; 7$	$PO_{10}; 7$

Table 2. Top 8 sensors for $C1_{SF}$, $C3_{SF}$, and $C4_{SF}$. Each cell represents the electrode position in the international EEG 10-20 system, and the number of times this electrode has been selected as one of the eight best sensors across the 20 subjects.

Table 2 presents the eight best sensors for $C1_{SF}$, $C3_{SF}$ and $C4_{SF}$. Each cell of the table represents the location of the sensor and the number of times where it was selected as one of eight best sensors across the 20 subjects. The eight best sensors of $C1_{SF}$ and $C3_{SF}$ share almost the same sensors. The only difference is CP_6 for $C1_{SF}$ and T_8 for $C3_{SF}$ but these two sensors are spatially very close. This similarity explains why the speller accuracies for these two criteria are so closed (cf. Fig 1).

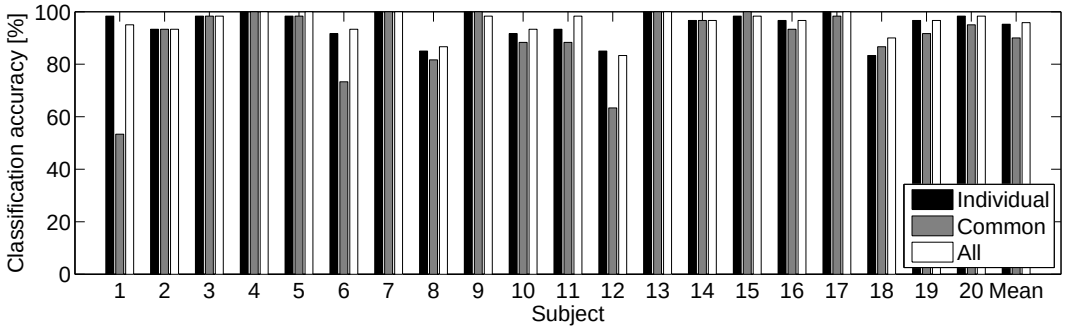


(a) Subject 1 (b) Subject 15 (c) Subject 16

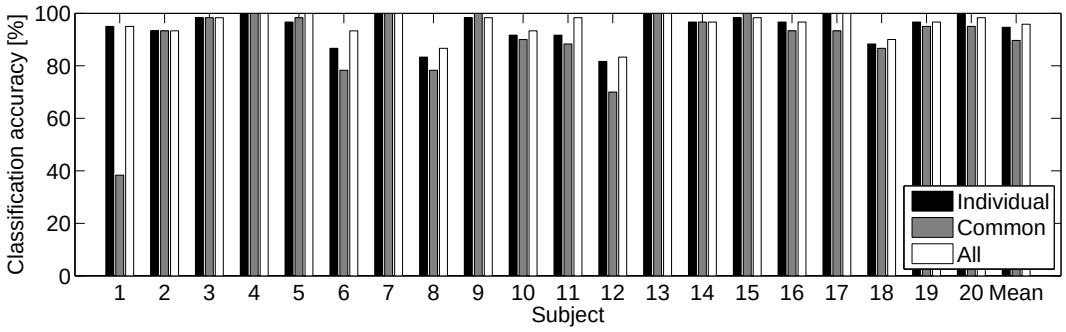
(d) Subject 1 (e) Subject 15 (f) Subject 16

Figure 7. Rank for every sensor (a), (b) and (c) ; P300 waves on the different sensors, starting after the flash and during 0.6s, based on estimated evoked potentials in $\hat{A}_1$ (d), (e) and (f).

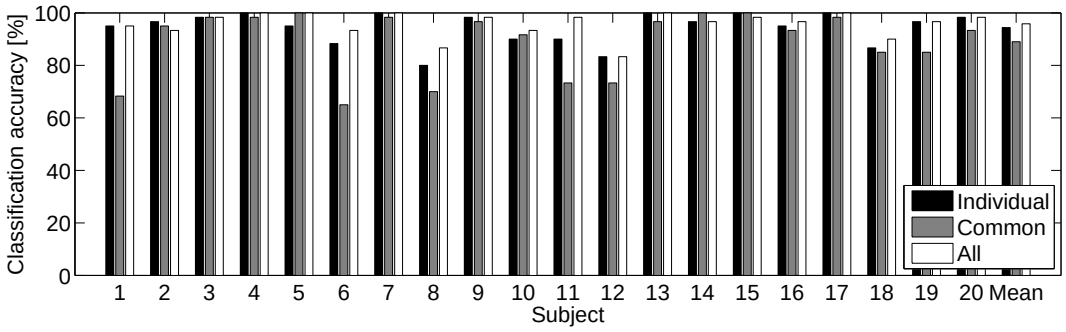
The comparison of the speller accuracy between the set of the eight best common sensors (common), the eight best sensors for each individual (individual), and the whole set of sensors (all, *i.e.,* with 32 sensors) in relation to each subject is presented in Fig. 8. These results correspond to the speller accuracy on the third test session with 10 epochs. The adaptive selection of the sensor subset provides usually the best results. It it particularly the case for Subject 1, 6 and 12. The sensor selection for Subject 1 is essential as the performance almost doubles. For several subjects (2, 3, 4, 13, 14), the accuracy is similar for the three sets of sensors.



(a) $C1_{SF}$ (Spatial filtering + SSNR evaluation)



(b) $C3_{SF}$ (Spatial filtering + P300 evaluation)



(c) $C4_{SF}$ (Spatial filtering + Speller evaluation)

Figure 8. Impact of the adaptive sensor selection (session 3, 10 epochs)

7. Discussion

7.1. Sensors location

Although the problem of feature selection is largely discussed topic in the pattern recognition literature, the problem of sensor selection in BCI and particularly for P300 based BCI has not been really explored. The classical approach for determining the best sensor selection is to chose a set among several predefined sets like in [18], where four sets of sensors were analyzed and compared. Contrary to this kind of approach, the proposed method allows determining the subsets without an a priori knowledge of the ideal sensor location.

The experiments have shown that it is possible to achieve relatively good

performance with only eight sensors chosen individually, with an accuracy of around 94% with 10 epochs. The analysis of the sensor rank obtained with $C1_{SF}$ (SSNR with spatial filters) suggests that several sensors are common to every subject. For the different subsets of eight sensors, which are personalized to each subject, five sensors are common to half of the subjects (P_z, P_8, O_z, P_3, P_7). One sensor is located on the occipital area, confirming previous works suggesting that occipital sites have also an important role [40, 18]. Although the P300 response has been discovered for over 40 years [41], its full understanding remains challenging and elusive [42]. The best locations for the sensors depend on the person and highlight both the complexity underlying the P300 process and the need of a personalized/adaptive P300-BCI.

7.2. Variation across subjects

The results described in section 6.4 suggest a certain reliability of the results over time. A performance drop between several sessions could be indeed a major drawback for commercial and/or clinical BCI applications. The variation across subjects could be an issue for creating an EEG cap, which would contain only a restricted number of electrodes placed at the occipital and parietal area. While it could provide a high performance for most of the subjects, it would be a drawback for people where the P300 response is easier to detect near the frontal area. A recent work based on demographic observations dealing with SSVEP-BCI has suggested that age and gender influence the performance [43]. The same way that EEG caps have different sizes and should be placed according to head measurements, the choice of a sensor sets for P300-BCIs would benefit from a demographic study where some well identified group of persons might need the same set of sensors [44, 45].

The proposed solution does not consider a specific criterion for stopping the backward elimination. It may be judicious to know when removing sensors depreciates the performance. Table 3 presents the correlation factor between the accuracy of the speller during the test and the evolution of the corresponding criterion in relation of the number of selected sensors. For a high correlation factor, it would be possible to set some thresholds that would provide some hints for stopping the backward elimination when a desired accuracy is required. For $C3$ and $C4$, the lack of spatial filters do not allow to find a high correlation between the speller accuracy and the criteria. For the other methods and particularly for $C1_{SF}$ and $C3_{SF}$, it would be possible to stop the backward elimination procedure in relation to a desired accuracy.

Criterion	$C1$	$C3$	$C4$	$C1_{SF}$	$C3_{SF}$	$C4_{SF}$
Correlation factor (5 epochs)	0.926	-0.896	-0.779	0.895	0.992	0.981
Correlation factor (10 epochs)	0.881	-0.878	-0.756	0.823	0.982	0.991

Table 3. Correlation between the criterion value and the classification accuracy.

A sensor selection step for each subject is essential and justified. When we consider adaptive subsets, the average performance with eight sensors is equivalent to the whole

set of 32 sensors. It can reduce the BCI cost and the time for preparing a user or a patient. Moreover, it is better to choose the sensor locations in relation to the subject. With a fixed sensor subset for every subject, Subject 1 would achieve poor performance. The average accuracy of the speller is higher with personalized sensor subsets than with a fixed predetermined subset.

In this paper, several questions have been answered for the sensor selection problem. A first outcome is the highlight of the unnecessary step of the speller evaluation. It is useless to base the strategy of the sensor subset evaluation on the speller accuracy. This is the last step in the different processing tasks leading to the recognition of letter from some EEG signal. The previous statement can be extended to the recognition of the P300 response, which is not needed either. The proposed method is based on the evaluation of the SSNR and provides equivalent results. The rawest evaluation of the signal provides the best sensor subsets. No direct information related to the P300 response was used for selecting the sensors, the only hypothesis is the presence of a response synchronized with the target stimuli. Thus, the proposed method could be adapted to other BCI paradigms for sensor selection like for motor imagery BCIs. In addition to its genericity, the computational task during the evaluation of the subsets is reduced.

8. Conclusion

Several strategies for the sensors subset evaluation of a P300-BCI speller have been evaluated. They were defined in relation to several points of view: the application aspect with the speller accuracy, the machine learning aspect with the P300 classification, and the signal processing aspect with the SSNR evaluation. The results clearly indicate that the best strategies always consider spatial filters as pre-processing. The two best methods are based on the evaluation of the SSNR and the P300 recognition, showing that it is useless to take into account the speller stage. While the SSNR and the P300 recognition provide both equivalent results, both consider spatial filters based on the xDAWN algorithm. Hence, the SSNR is directly computed during the creation of the spatial filters whereas the P300 classification requires several training and testing. This reveals the sufficiency of the evaluation of the SSNR preceded by spatial filtering for creating suboptimal sets of sensors, *i.e.,* suboptimal sets of features for the classifier. Finally, as the SSNR and spatial filtering can be both obtained in the same procedure, it reinforces the choice of the proposed strategy. It allows avoiding further processing while keeping good performance.

Acknowledgment

This work has been supported by French National Research Agency (ANR) through TecSan program (project RoBIK ANR-09-TECS-013) and through DEFIS program (project Co-Adapt ANR-09-EMER-002).

Appendix A.

This appendix describes the different steps for computing the SSNR of the signal after spatial filtering and how to determine the spatial filters. In the definition of the SSNR defined in section 4, we replace $\hat{A}_1$ by $B_1^T X$ where B_1^T is a part of the least mean square estimation Eq. (6). Then, we apply a QR decomposition on $D_1 = Q_1 R_1$ and $X = Q_x R_x$. Finally, one can express Eq. (10) as:

$$\text{SSNR}(V_1) = \frac{Tr(V_1^T (Q_x^T B_1 R_1^T R_1 B_1^T Q_x) V_1)}{Tr(V_1^T V_1)}, \tag{A.1}$$

where $V_1 = R_x U_1$. V_1 is therefore obtained from the Rayleigh quotient, whose solution is the concatenation of N_f eigenvectors associated with the N_f largest eigenvalues of $Q_x^T B_1 R_1^T R_1 B_1^T Q_x$ [46]. These vectors are estimated thanks to a singular value decomposition (SVD) of $R_1 B_1^T Q_x = \Phi \Lambda \Psi^T$, Φ and Ψ being two orthogonal matrices and Λ being a diagonal matrix with nonnegative diagonal elements in decreasing order.

After simplification, we obtain:

$$\text{SSNR}(V_1) = \frac{Tr(V_1^T (\Psi \Lambda^2 \Psi^T) V_1)}{Tr(V_1^T V_1)}. \tag{A.2}$$

By considering again the Rayleigh quotient for V_1, the associated solution corresponds to the N_f largest eigenvalues of $\Psi \Lambda^2 \Psi^T$, which are Λ^2. In addition, the denominator can be easily simplified to the trace of the identity of size $N_f \times N_f$, as Ψ and Q_x are orthogonal matrices. Therefore, the SSNR of the enhanced signal, *i.e.,* after spatial filtering, can be defined by:

$$\text{SSNR} = Tr(\Lambda^2)/N_f. \tag{A.3}$$

The solution of Eq. (11) provides the spatial filters, which are ordered in decreasing order by relevance impact.

$$\hat{U}_1 = R_x^{-1} \Psi. \tag{A.4}$$

References

[1] B. Z. Allison, E. W. Wolpaw, and J. R. Wolpaw. Brain-computer interface systems: progress and prospects. *Expert Review of Medical Devices*, 4(4):463–474, 2007.

[2] N. Birbaumer and L. G. Cohen. Brain-computer interfaces: communication and restoration of movement in paralysis. *Journal of Physiology-London*, 579(3):621–636, 2007.

[3] H. Cecotti, I. Volosyak, and A. Gräser. Evaluation of an SSVEP based brain-computer interface on the command and application levels. *4th IEEE EMBS International Conference on Neural Engineering*, 2009.

[4] E. I. Shih, A. H. Shoeb, and J. V. Guttag. Sensor selection for energy-efficient ambulatory medical monitoring. *In Proc. of the 7th International Conference on Mobile Systems, Applications and Services*, pages 347–358, 2009.

[5] B. Blankertz, G. Dornhege, S. Lemm, M. Krauledat, G. Curio, and Klaus-Robert Müller. The Berlin brain-computer interface: EEG-based communication without subject training. *IEEE Trans. on Neural Systems and Rehabilitation Engineering*, 14(2):147–152, 2006.

[6] F. Lotte, M. Congedo, A. Lecuyer, F. Lamarche, and B. Arnaldi. A review of classification algorithms for EEG-based brain-computer interfaces. *Journal of Neural Engineering*, 4:R1–R13, 2007.

[7] K.-R. Müller, M. Krauledat, G. Dornhege, G. Curio, and B. Blankertz. Machine learning techiques for brain-computer interfaces. *Biomed Tech*, 49(1):11–22, 2004.

[8] K.-R. Müller, M. Tangermann, G. Dornhege, M. Krauledat, G. Curio, and B. Blankertz. Machine learning for real-time single-trial EEG-analysis: From brain-computer interfacing to mental state monitoring. *J Neurosci Methods*, 167(1):82–90, 2008.

[9] C. W. Anderson, S. V. Devulapalli, and E. A. Stolz. Determining mental state from EEG signals using parallel implementations of neural networks. *IEEE Workshop on Neural Networks for Signal in Processing, Cambridge, MA, USA,*, pages 475–483, 1995.

[10] H. Cecotti and A. Gräser. Convolutional neural networks for P300 detection with application to brain-computer interfaces. *IEEE Trans. Pattern Analysis and Machine Intelligence*, 2010.

[11] T. Felzer and B. Freisieben. Analyzing EEG signals using the probability estimating guarded neural classifier. *IEEE Trans. on Neural Systems and Rehab. Eng.*, 11(4), 2003.

[12] E. Haselsteiner and G. Pfurtscheller. Using time dependent neural networks for EEG classification. *IEEE Trans. Rehab. Eng.*, 8(4):457–463, 2000.

[13] N. Masic and G. Pfurtscheller. Neural network based classification of single-trial EEG data. *Artificial Intelligence in Medicine*, 5(6):503–513, 1993.

[14] N. Masic, G. Pfurtscheller, and D. Flotzinger. Neural network-based predictions of hand movements using simulated and real EEG data. *Neurocomputing*, 7(3):259–274, 1995.

[15] B. Blankertz, G. Curio, and K.-R. Müller. Classifying single trial EEG: Towards brain computer interfacing. *In T. G. Diettrich, S. Becker, and Z. Ghahramani, editors, Advances in Neural Inf. Proc. Systems (NIPS 01)*, 14:157–164, 2002.

[16] A. Rakotomamonjy and V. Guigue. BCI competition iii : Dataset ii - ensemble of SVMs for BCI P300 speller. *IEEE Trans. Biomedical Engineering*, 55(3):1147–1154, 2008.

[17] U. Hoffmann, J. M. Vesin, K. Diserens, and T. Ebrahimi. An efficient P300-based brain-computer interface for disabled subjects. *Journal of Neuroscience Methods*, 167(1):115–125, 2008.

[18] D. J. Krusienski, E. W. Sellers, D.J. McFarland, T. M. Vaughan, and J. R. Wolpaw. Toward enhanced P300 speller performance. *Journal of Neuroscience Methods*, 167:15–21, 2008.

[19] B. Obermaier, C. Guger, C. Neuper, and G. Pfurtscheller. Hidden markov models for online classification of single trial EEG data. *Pattern Recognition Letters*, 22(12):1299–1309, 2001.

[20] S. Zhong and J. Gosh. HMMs and coupled HMMs for multi-channel EEG classification. *In Proc. IEEE Int. Joint. Conf. on Neural Networks*, 2:1154–1159, 2002.

[21] *Algorithms and Theory of Computation Handbook*. CRC Press LLC, 1999.

[22] T. N. Lal, M. Schroder, T. Hinterberger, J. Weston, M. Bogdan, N. Birbaumer, and B. Scholkopf. Support vector channel selection in bci. *IEEE Trans. Biomed. Engineering*, 51(6):1003–1010, 2004.

[23] M. Schroder, T. N. Lal, T. Hinterberger, M. Bogdan, J. N. N. Jeremy Hill, N. Birbaumer, W. Rosenstiel, and B. Schoolkopf. Robust eeg channel selection across subjects for brain-computer interfaces. *EURASIP Journal on Applied Signal Processing*, 19:3103Ű3112, 2005.

[24] L. Farwell and E. Donchin. Talking off the top of your head: toward a mental prosthesis utilizing event-related brain potentials. *Electroencephalogr. Clin. Neurophysiol.*, 70:510–523, 1988.

[25] E. Donchin, K. M. Spencer, and R. Wijesinghe. Assessing the speed of a P300-based brain-computer interface. *IEEE Trans. Neural Sys. Rehab. Eng.*, 8(2):174–179, 2000.

[26] N. Abe, M. Kudo, J. Toyama, and M. Shimbo. Classifier-independent feature selection on the basis of divergence criterion. *Pattern Anal. Appl.*, 9(2):127–137, 2006.

[27] D. J. C. MacKay. Bayesian interpolation. *Neural Comput.*, 4(3):415–447, 1992.

[28] G. R. Müller-Putz, R. Scherer, C. Brauneis, and G. Pfurtscheller. Steady-state visual evoked potential (SSVEP)-based communication: impact of harmonic frequency components. *Journal of Neural Engineering*, 2(1):123–130, 2005.

[29] N. Xu, X. Gao, B. Hong, X. Miao, S. Gao, and F. Yang. BCI competition 2003–data set iib: enhancing P300 wave detection using ICA-based subspace projections for BCI applications. *IEEE Trans Biomed Eng*, 51(6):1067–1072, 2004.

[30] B. Blankertz, M. Kawanabe, R. Tomioka, F. Hohlefeld, V. Nikulin, and K.-R. Müller. Invariant common spatial patterns: Alleviating nonstationarities in brain-computer interfacing. *Advances in Neural Information Processing Systems*, 20, 2008.

[31] C. Brunner, M. Naeem, R. Leeb, B. Graimann, and G. Pfurtscheller. Spatial filtering and selection of optimized components in four class motor imagery EEG data using independent components analysis. *Pattern Recognition Letters*, 28(8):957–964, 2007.

[32] M. Congedo, F. Lotte, and A. Lécuyer. Classification of movement intention by spatially filtered electromagnetic inverse solutions. *Physics in Medicine and Biology*, 51:1971–1989, 2006.

[33] G. Pfurtscheller, C. Guger, and H. Ramoser. EEG-based brain-computer interface using subject-specific spatial filters. *International Work-Conference on Artificial and Natural Neural Networks,*, 2:248–254, 1999.

[34] R. Tomioka, N. J. Hill, B. Blankertz, and K. Aihara. Adapting spatial filter methods for nonstationary BCIs. *Workshop on Information-Based Induction Sciences (IBIS), 6*, 2006.

[35] O. Friman, I. Volosyak, and A. Gräser. Multiple channel detection of steady-state visual evoked potentials for brain-computer interfaces. *IEEE Trans. Biomed. Eng.*, 54(4):742–750, 2007.

[36] B. Rivet, A. Souloumiac, G. Gibert, and V. Attina. P300 speller brain-computer interface: Enhancement of P300 evoked potential by spatial filters. *In Proc. EUSIPCO*, 2008.

[37] B. Rivet, A. Souloumiac, V. Attina, and G. Gibert. xDAWN algorithm to enhance evoked potentials: application to brain-computer interface. *IEEE Trans Biomed Eng.*, 56(8), 2009.

[38] E. Maby, G. Gibert, P.-E. Aguera, M. Perrin, O. Bertrand, and J. Mattout. The OpenViBE P300-Speller scenario: a thorough online evaluation. *In Human Brain Mapping Conference*, 2010.

[39] G. E. Chatrian, E. Lettich, and P. L. Nelson. Ten percent electrode system for topographic studies of spontaneous and evoked EEG activity. *Am J EEG Technol*, 25:83–92, 1985.

[40] H. Cecotti and A. Gräser. Time delay neural network with Fourier Transform for multiple channel detection of steady-state visual evoked potential for brain-computer interfaces. *In Proc. EUSIPCO*, 2008.

[41] S. Sutton, M. Braren, J. Zubin, and E. R. John. Evoked potential correlates of stimulus uncertainty. *Science*, 150:1187–1188, 1965.

[42] J. Polich. Updating P300: An integrative theory of P3a and P3b. *Clinical Neurophysiology*, 118:2128–2148, 2007.

[43] B. Z. Allison, T. Lüth, D. Valbuena, A. Teymourian, I. Volosyak, and A. Gräser. BCI demographics: How many (and what kinds of) people can use an SSVEP BCI? *IEEE Trans Neural Syst Rehabil Eng*, 18(2):107–116, 2010.

[44] C. Guger, G. Edlinger, W. Harkam, I. Niedermayer, and G. Pfurtscheller. How many people are able to operate an EEG-based brain-computer interface (BCI)? *IEEE Trans. Neural Syst Rehabil Eng.*, 11(2):145–147, 2003.

[45] C. Guger, S. Daban, E. Sellers, C. Holznera, G. Krausza, R. Carabalonac, F. Gramaticac, and G Edlinger. How many people are able to control a P300-based brain.computer interface (BCI)? *Neuroscience Letters*, 462:94–98, 2009.

[46] G. H. Golub and C. F. Van Loan. *Matrix Computations*. 3rd ed. Johns Hopkins University Press, 1996.